International Journal of Anatomy and Research,
Int J Anat Res 2024, Vol 12(4):9085-92. ISSN 2321-4287
DOI: https://dx.doi.org/10.16965/ijar.2024.237

Original Research Article

Fractal Analysis of Chest Radiographs Using Image-J-FIJI Software- A Pilot Study

Pooja I Shettannavar [1], Dishitha Kopoori [2], Vivek Chail [3], Vasudha Kulkarni [4].

[1] Postgraduate, Department of Radiodiagnosis, Dr. B. R. Ambedkar Medical College and Hospital, Kadugondanahalli, Bengaluru, Karnataka, India.

[2] Medical Student, Akash Institute of Medical Sciences and Research Centre, Bangalore, Karnataka, India.

[3] Professor, Department of Radiodiagnosis, Dr. B.R. Ambedkar Medical College and Hospital Kadugondanahalli, Bengaluru, Karnataka, India.

[*4] Professor and HOD, Department of Anatomy, Akash Institute of Medical Sciences and Research Centre, Bangalore, Karnataka, India.

ABSTRACT

Background: Lung vasculature has nutritive and functional roles. Unlike the bronchial tree which branches dichotomously into twenty-one generations, the pulmonary arteries give supernumerary branches to perfuse the neighboring parenchyma. The pulmonary arteries additionally branch for five more generations than airways before forming capillaries. Further pulmonary veins are interlobular in position. Hence the characterization quantifying the pulmonary vascular networks is challenging.

Objective: In this study, we assessed the pulmonary vasculature in chest radiographs using the fractal analysis method on Image-J-Fiji software.

Design: Cross-sectional study **Settings:** Patients referred to the Department of Radiodiagnosis, Akash Institute of Medical Sciences and Research Centre and Dr. B. R. Ambedkar Medical College, Bangalore, Karnataka, India.

Participants: One hundred and thirty-two chest radiographs of normal healthy individuals (aged 2 months to 80 years) were photographed. Each of these images was processed in the Image-J-Fiji software. A box-counting algorithm quantified the images. Data results of the fractal dimensions were validated at the probability of significance [0.05].

Results: The mean fractal dimension of the pulmonary vasculature was 1.39. For males and females, the Pearson's correlation coefficient between the fractal dimension and age in years was 0.102 and 0.16, respectively. In males, a chi-square value of 0.58, in females, a chi-square value of 1.03, degree of freedom 2 and critical value of p-value 0.05, showed the relation was statistically not significant. Comparison between fractal dimension and Gender using Cramer's V test in males, 0.066, and in females, 0.088, indicates a weak association between fractal dimension and gender.

Conclusion: The applicability of the fractal dimensions is to screen the high risks of severe chronic obstructive pulmonary diseases. The determination of fractal values helps evaluate the complexity of lung tumors. The baseline data concerning fractal properties of pulmonary vasculature obtained from this study helps to evaluate lung diseases like emphysema and vascular abnormalities during the progression of chronic obstructive pulmonary disease.

KEYWORDS: Chest Radiograph, Image Analysis, Fractal dimension, Pulmonary vasculature.

Corresponding Author: Dr. Vasudha Kulkarni, Professor and HOD, Department of Anatomy, Akash Institute of Medical Sciences and Research Centre, Bangalore, Karnataka, India.

E-Mail: vasu_anil77@rediffmail.com

Access this Article online	Journal Information
Quick Response code	**International Journal of Anatomy and Research** ISSN (E) 2321-4287 | ISSN (P) 2321-8967 **https://www.ijmhr.org/ijar.htm** **DOI-Prefix:** https://dx.doi.org/10.16965/ijar
	Article Information
DOI: 10.16965/ijar.2024.237	Received: 07 Nov 2024 Peer Review: 08 Nov 2024 Revised: 15 Nov 2024 Accepted: 29 Nov 2024 Published (O): 05 Dec 2024 Published (P): 05 Dec 2024

INTRODUCTION

Numerous vascular and neural networks in the human body support proper physical function. The capillary network of the lungs is one such example of a complex network. The bronchial artery provides nutrition, and the functional vasculature starts in the pulmonary artery, which gets nonoxygenated blood from the right ventricle. It is difficult to evaluate pulmonary networks because these complex networks cannot be comprehended through the use of conventional geometry. Therefore, while assessing such complex networks, the fractal notion is helpful [1].

Pulmonary vascular pathology encompasses a remarkable range of acquired and congenital disorders. Diagnostic imaging is necessary to plan further management for disorders involving pulmonary vasculature, such as pulmonary hypertension with lung disease/hypoxemia, chronic obstructive pulmonary disease (COPD), interstitial lung diseases, sleep disorders, alveolar hypoventilation disorders, chronic thromboembolic pulmonary hypertension, systemic disorders (such as sarcoidosis and lymphangioleiomyomatosis), metabolic disorders (such as thyroid disorders or glycogen storage diseases), and other causes (such as chronic renal failure and segmental pulmonary hypertension). A helpful metric for describing the spatial pattern of pulmonary vascular disease progression and forecasting clinical outcomes in these circumstances is the fractal dimension. Chest radiography, ultrasound, magnetic resonance imaging (MRI), computed tomography (CT), ECG-gating detailed imaging of the pulmonary vein ostia, and other imaging modalities are available to help evaluate the pulmonary vasculature [2]. A deeper comprehension of the structural changes that occur during the prognosis of pulmonary diseases may result from fractal analysis of the parenchyma and airways, particularly when paired with computer simulations [3].

METHODS

Source of data: Chest radiographs available in the medical record department of Akash Institute of Medical Sciences and Research Centre, Bangalore, and Dr. B. R. Ambedkar Medical College Karnataka, India. After obtaining ethical clearance, a total of 132 chest radiographs (47 females and 85 males) of normal healthy individuals aged 2 months of an infant to 80 years were photographed. The acquired radiographs were then processed in the Image-J-Fiji software and were quantified by a box-counting algorithm [2,4]. Chest radiographs showing any lung and cardiac pathology such as bronchiectasis, lung carcinoma, pleural effusion, bronchopneumonia, chronic obstructive pulmonary disease, atelectasis, dilated cardiomyopathy, cardiomegaly, congestive cardiac failure, any congenital chest disorders such as kyphoscoliosis were excluded. The image was transformed into a binary 8-bit image as a processing step before analysis **(Fig 1)**.

Then the image was skeletonized **(Fig 2)**. The box-counting method was applied to estimate the fractal dimension (FD) of a 2D Gray-level image. Using the regression plot between log(N) and log(1/r), the fractal dimension was computed. The graph was a log-log plot of the minimum number of squares (Log(number)) required to cover the edges of the binarized image against the side value of the identical squares (log(Cn)). The optimal regression line was displayed together with the pertinent 95% Class Interval **(Fig 3)**.

The statistical differences were analyzed using SPSS version 26 software. To ascertain whether there was a statistically significant difference between the study population's age and fractal dimension, gender, and fractal dimension value, Pearson correlation and Chi-square test were applied.

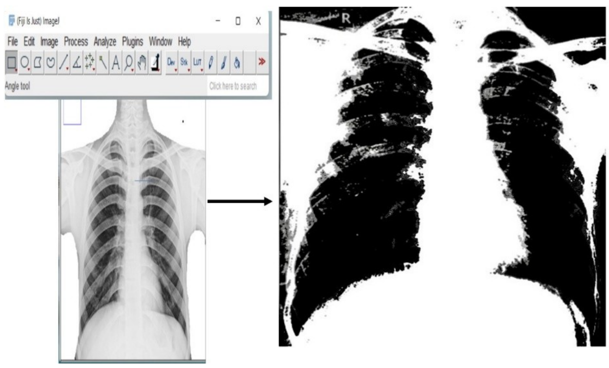

Fig. 1: Image preprocessing; Image is converted into 8 bit image in tiff format

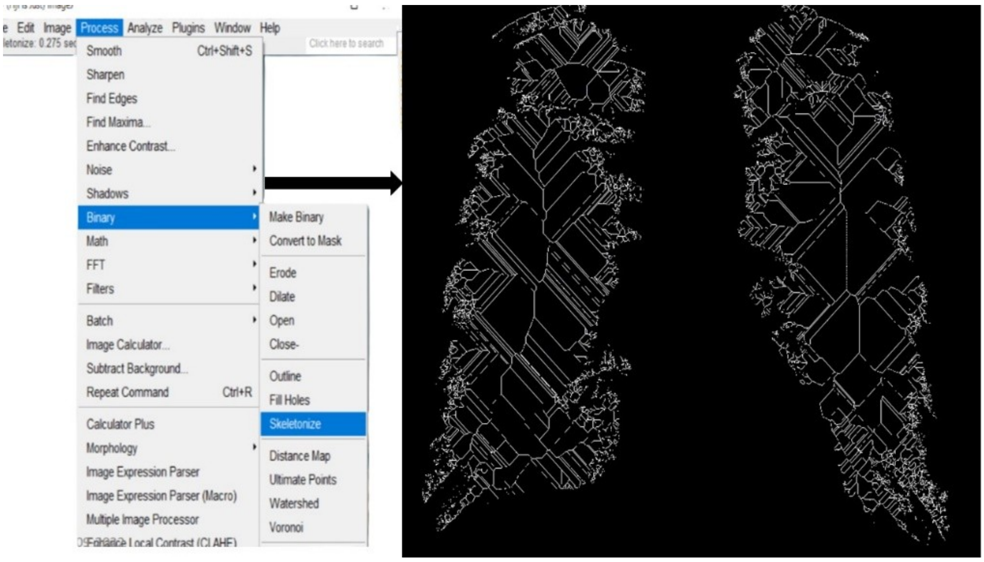

Fig. 2: 8 bit image is processed for binarization and skeletonization.

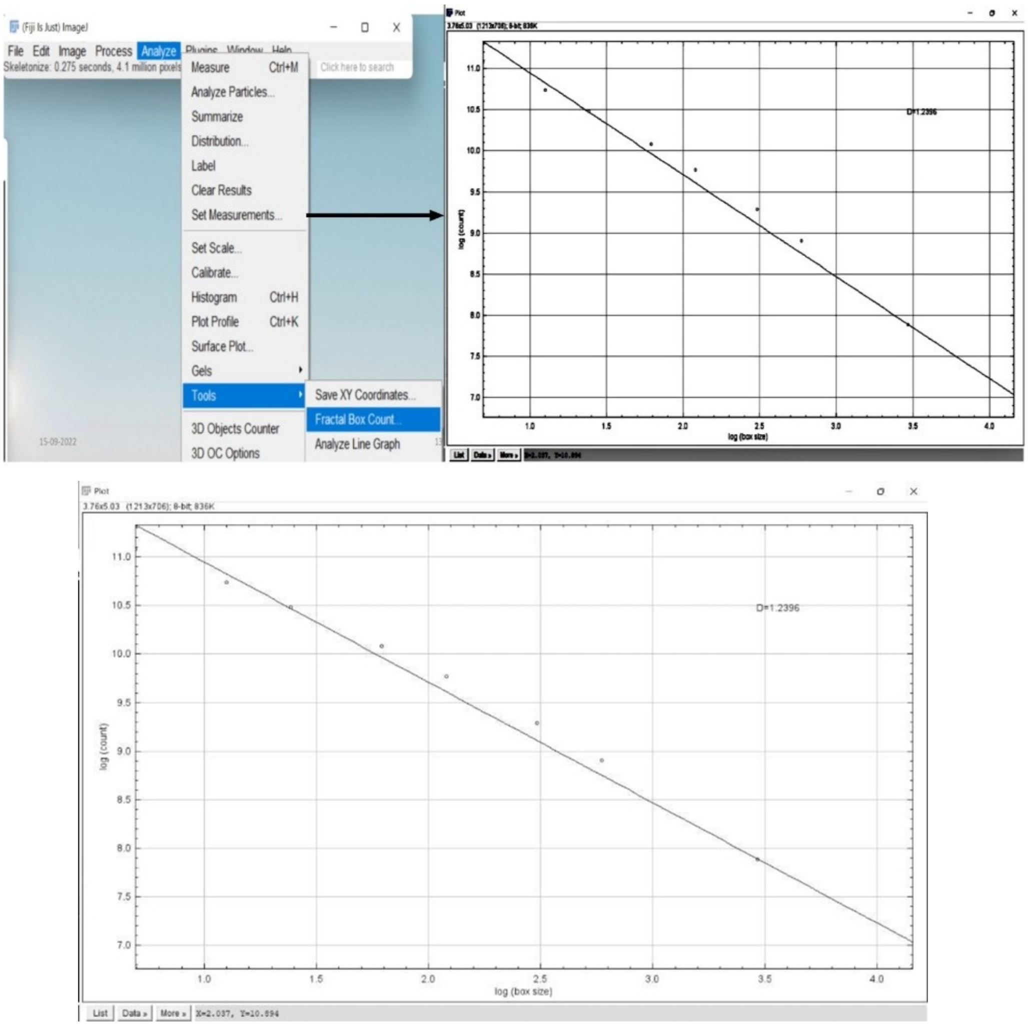

Fig. 3: The image is analysed by using fractal box-count tool.

RESULTS

The age range of the study participants was 2 months to 80 years, with 64.4% of the participants being male and 35.6% being female. The mean fractal dimension values are shown in **Table 1.** The Pearson's correlation coefficient between Mean fractal dimension and Age in years was 0.114. For males and females, the Pearson's correlation coefficient between the fractal dimension and age in years was 0.102 and 0.16, respectively, indicating that fractal dimension values do not rise noticeably with age. A chi-square test was conducted to find an association between fractal dimension and gender. In males, a chi-square value of 0.58, in females, a chi-square value of 1.03, degree of freedom 2 and critical value of p-value 0.05, showed the relation was statistically not significant. Comparison between fractal dimension and Gender using Cramer's V test in males, 0.066, and in females, 0.088, indicates a weak association between fractal dimension and gender.

Table 1: Comparison of age with fractal Dimension of the Study Population.

	Age (in years)	FD value Males	FD value Females
Maximum	80	1.63	1.57
Minimum	0.2	1.18	1.19
Mean	37	1.39	1.39

DISCUSSION

Benoit Mandelbrot defined fractal geometry (1924-2010). It is used in a variety of fields, including medicine to measure dendritic branching patterns and the meteorological department to evaluate coastlines. If an object demonstrates the self-similarity property across various assessment length scales, it is said to form a fractal. A potent technique for the morphological characterization of intricate systems, fractal analysis is extensively used in biomedical images. For the multiscale level of tissue structure discrimination, spatial resolution and image segmentation are essential [1]. Fractal geometry has been extensively studied in several areas related to pattern detection and image analysis of neural networks, pulmonary vascular networks, and retinal ganglion cells. A comparison of fractal dimension values from previous studies revealed that our findings were similar to the fractal dimension values of an earlier study by De-Giorgio et al., 2022 **(Table 2)**.

High-resolution X-ray phase-contrast micro-tomography (XrPCìT) images of both i njured and uninjured tissue of a mouse spinal cord were subjected to fractal analysis in a study by Maugeri L et al [5].

The fractal dimension was estimated using the box- counting method on tomographic slices segmented at different threshold levels. Regardless of the criterion that was used, this study found that the ipsilateral damaged hemicord had a higher fractal dimension than the contralateral intact tissue. The calculation of the fractal dimension was heavily reliant on the image histogram, or the distribution of pixel intensity in the photos. Specifically, a changed neuron/glia ratio—possibly brought on by neuronal loss and/or the recruitment or activation of glial cells (i.e., reactive astrocytes and microglia)—could have contributed to the enhanced fractal dimension in the damaged hemicord. The findings provide methodological approaches that may be helpful for XrPCìT picture fractal dimension analysis, which aims to assess topological complexity and identify structural alterations in biological tissues [5].

Using MATLAB R2017a software and the box-count approach, Nichita MV et al. examined a lung radiograph to ascertain the fractal dimension of the pulmonary artery branching pattern. There was no statistically significant difference between the fractal dimension values obtained using the Harmonic and Fractal Image Analyzer program (D=1.5661+/-0.11691) and the MATLAB environment (The fractal dimension = 1.7086 +/- 0.17389) [2].

The study by Jelinek HF et al [4] allowed us to compare how the fractal dimension values determined by various approaches may vary and how fractal analysis may be effective for retinal ganglion cell characterization since there are numerous useful methods for computing fractal dimensions. Data from 192 previously published retinal neuron images was gathered for this purpose, and each image was examined in three different ways: as skeletonized tracings, binary or actual drawings (black-on-white), and as border images that were one pixel wide. Calliper, box-counting, mass-radius, dilation, and cumulative intersection methods were among the algorithms based on Hausdorff and Minkowski-Bouligand dimensions. Finding the relationship between an image's mass or length and changes in the measure's scale was the foundation of every fractal analysis technique covered in this work. Retinal

Table 2: Comparison of fractal dimension with previous studies.

Sl no	Author, Year	Method of fractal analysis	Data of Images	Mean fractal dimension values
1	Family et al., 1989 [7]	Mass-radius relation and two point correlation	Retinal vessels in human	1.71
2	Landini et al., 1993 [8]	Box counting algorithm	Fluorescein angiogram of retina in humans	1.76
3	Caserta et al., 1994 [9]	Cumulative-mass method Sholl analysis	Images of Retinal ganglion cells	1.63
4	Landini at al., 1995 [8]	Mass radius relation and two-point correlation	Fluorescein angiogram Fundus	1.26
5	Bordescu et al ., 2018 [10]	Differential box-counting method	MRI Brain in Alzheimer's disease	1.5-1.6
6	Paun VP et al., 2018 [14]	Standard box-counting method using MATLAB R2017a	X-Ray Lung Arterial network	1.56
7	Nichita MV et al.,, 2018 [2]	Standard box-counting method using MATLAB R2017	X-Ray Lung vascular network	1.7
8	Nichita MV et al., 2020 [15]	Altered box-counting method using MATLAB R2017	X-Ray Lung vascular network	1.65
9	De-Giorgio et al., 2022 [12]	Box counting method using ImageJ	Post mortem CT scan Brain	1.2-1.9
10	Present study, 2024	Box Counting method using Image-J-Fiji software	X-Ray Lung vasculature	1.39

ganglion cell classification utilizing Scheffe and Analysis of Variance (ANOVA) for repeated measures for identical cell groups, the Post Hoc test for matched pairs to examine mean differences revealed statistical differences in their observed FD values ($p<0.001$) [4].

The topology of the neuron tracts in the human brain has been determined using the tractography pictures generated by magnetic resonance imaging scans. Lacunarity was calculated using the Gliding Box method to evaluate the level of clustering in the neural tracts network. Using Diffusion Tensor Imaging (DTI) Tractography pictures, Katsaloulis P et al.'s study [6] sought to examine the structural complexity of textures originating from healthy areas of the brain and quantify the structural complexity of brain neuronal axons. Fractal dimensions ranged from 1.58 to 1.6 on average. It was evident that the neuron tracts do not uniformly cover the entire brain region and that the tractography images were fractals. The length of the neuron tract networks and the space they occupy appeared to follow scaling principles, and their structure was statistically scale-invariant. These findings suggested that the fractal architectures of the brain's neural pathways might resemble those of other biological tissues, including arteries, bronchial trees, and retinal ganglion cells [6].

To ascertain whether retinal vessels have a fractal structure, the mechanism underlying the formation of retinal vessel patterns in the developing human eye was investigated using one fluorescein angiogram of the human retina and six red-free (30x30 cm) photographs (the blood vessels are enhanced by a green 540 nm cutoff filter). The fractal dimension of the retina circulation patterns was ascertained using the mass-radius approach and the two-point correlation function method. Using the mass-radius and two-point correlation function approaches, the mean value of the fractal dimension was 1.7 [7].

Landini G et al looked into the locally connected fractal dimension because the generalized box fractal dimension was unable to distinguish between normal and pathological retinal arteries in 60° fluorescein angiograms. Twenty-four digitized 60° fluorescein angiograms of individuals with normal retinas and five angiograms of patients with central retinal vein or artery occlusion were examined. The local complexity of the angiography was assessed using the point-wise technique inside a limited window which was centered on the pixels that were part of the retinal arteries. The study concluded that local retinal vascular anomalies might be objectively characterized and detected automatically using this technology [8].

For many years, quantitative morphological examinations of the dendritic arborizations of neurons have been conducted using the Sholl analysis approach. Fractal analysis (cumulative-mass approach) can average away noise, resulting in a more accurate depiction of the neuron, according to a comparison of Sholl and fractal analysis. This work by Caserta F et al. [9] showed that the fractal dimensions of the three types of cat retinal ganglion cells varied when they were examined. Tonic W cells' fractal dimensions were more comparable to X cells' values. Cat retinal ganglion cells were the most diverse, as evidenced by the phasic W cells that were examined having the greatest variation in fractal dimensions. Additionally, the apparent complexity of dendritic arborizations of neurons in two and three dimensions can be morphometrically characterized using fractal dimensions [9].

To distinguish between benign and malignant tissues and to categorize the many brain morphologies displayed by formatting cell lines, lacunarity, an additional metric frequently utilized in conjunction with fractal dimension was used to characterize the texture of a shape or fractal [6]. Bordescu D et al., created the technique that estimates the fractal dimension and lacunarity and was used to discover structures linked to Alzheimer's disease. With a tiny margin removed from the remaining tissue using the differential box-counting approach, the normal physiological brain zone was regarded as the benign area, the entire mixed zone as the biphasic region, and the tumor itself as the lacunarity area, respectively. Though it met more lacunarity than biphasic tissue, the lacunarity tissue tended to have a similar fractal dimension [10].

For the examination of magnetic resonance images, fractal analysis is suitable. Using fractal analysis, three modified algorithms (piecewise-threshold-box counting, the enhanced piecewise-modified-box-counting (PMBC), and piecewise-triangular prism-surface-area (PTPSA) methods) were presented for tumor identification, along with a description of the current fractal-based strategies. The PMBC algorithm was more sensitive and provided superior results in identifying and locating the tumor when compared to the PTPSA approach [11].

The temporal change of the average fractal dimension value was examined in the brains of four people whose time of death was known. It showed promise for use in quantitatively tracking post-mortem changes over time, as the average fractal dimension calculated on each brain slice showed a consistent trend across subjects. The analysis was expanded by examining the fluctuation in fractal dimension as a function of the various threshold levels used over time since it is sensitive to the threshold used for the binarized image. This approach yielded a collection of reliable quantitative parameters that may be connected to the time of death in more in-depth research on the early and late phases of a corpse's decomposition process [12].

Kido S et al. [13] employed high-resolution CT scans with fractal analysis from 70 patients with bronchogenic carcinomas and 47 patients with benign pulmonary nodules to examine the lung-nodule interfaces on small peripheral pulmonary nodules (less than 2 cm). The box-counting technique was employed for binary and grayscale nodule images to calculate the fractal dimensions. Compared to other nodules, hamartomas had reduced fractal dimensions ($P < 0.05$). Compared to bronchogenic carcinomas and hamartomas, the fractal dimensions derived from the grayscale images of pneumonia and tuberculoma were larger. Fractal dimensions of adenocarcinomas were higher than those of squamous cell carcinomas in bronchogenic carcinomas ($P < 0.05$). The study concluded that the features of the lung-nodule interfaces of small peripheral pulmonary nodules were reflected in the fractal dimensions. The complexity of the diverse textures and the imperfections of the curves were made visible by the fractal dimensions. It was possible to differentiate between benign lung nodules and bronchogenic carcinomas by using fractal dimension [13].

The drawback of the box-counting method, in particular, is that it requires determining the smallest number of boxes of a certain size that cover the item to provide an objective estimate of fractal dimension. Offsetting the original grid's origin can accomplish this, but it takes a long time and has an error rate of less than 0.5% [6].

CONCLUSION

The fractal dimension summarises concisely the amount of detail and complexity of pulmonary vasculature. While simple measurements of areas and volumes of pulmonary vasculature and disease pathology of airway structure are common, these methods do not capture the structural complexity of the lung. Since fractals have been successfully applied to evaluate complexity, this study would aid in describing the fractal properties of pulmonary vascular disease, emphysema, and vascular abnormalities in chronic obstructive pulmonary disease. The study suggests that fractal dimension values can be an objective and useful parameter to characterize the morphological complexity of pulmonary vasculature.

ORCiD

Pooja I Shettannavar – 0009-0001-1366-0732
Dishitha Kopoori – 0009-0001-7067-9544
Vivek Chail – 0000-0003-1170-0646
Vasudha Kulkarni – 0000-0002-2079-0244

Author Contributions

Concept and design of study: Vasudha Kulkarni. Acquisition of data: Dishitha Kopoori, Vivel Chail. Analysis and interpretation of data: Dishitha Kopoori, Vasudha Kulkarni. Drafting the article: Pooja Shettannavar, Vasudha Kulkarni. Revising it critically for important intellectual content: Vivek Chail, Vasudha Kulkarni. Final approval of the version to be published: Vasudha Kulkarni.

ACKNOWLEDGEMENTS

We extend our heartfelt gratitude to the management, the esteemed principal, and the faculty of the anatomy and radiology department for their support and guidance throughout the research process. We also would like to thank Ms. Manjula, our statistician for assistance in the statistical analysis of the study. Additionally, we extend our thanks to the International Journal of Anatomy and Research, for providing us with a platform to share our findings and insights.

Conflicts of Interests: None

REFERENCES

[1]. Mandelbrot B. Fractal geometry of nature. Freeman, New York 1983; 25-57.

[2]. Nichita MV, Paun VP. Fractal analysis in Complex Arterial Network of Pulmonary X-ray images. Scientific Bulletin-University Politehnica of Bucharest 2018 Apr;80(2):325-339.

[3]. Tanabe N, Sato S, Suki B, Hirai T. Fractal Analysis of Lung Structure in Chronic Obstructive Pulmonary Disease. Frontiers Media SA 2020 Dec ;11:1-11. https://doi.org/10.3389/fphys.2020.603197 PMid:33408642 PMCid:PMC7779609

[4]. Jelinek HF, Fernández E. Neurons and fractals: how reliable and useful are calculations of fractal dimensions?. Elsevier 1998 Jun ;81(1) 9-18. https://doi.org/10.1016/S0165-0270(98)00021-1 PMid:9696304

[5]. Maugeri L, DiNuzzo M, Moraschi M, Nicaise C, Bukreeva I, Mangini F, Giove F, Cedola A, Fratini M. Fractal Dimension Analysis of High-Resolution X-Ray Phase Contrast Micro-Tomography Images at Different Threshold Levels in a Mouse Spinal Cord. Multidisciplinary Digital Publishing Institute 2018 Dec;3(4): 1-11. https://doi.org/10.3390/condmat3040048

[6]. Katsaloulis P, Verganelakis DA, Provata A. Fractal dimension and lacunarity of tractography images of the human brain. World Scientific Publishing Company 2009 Jun ;17(2): 1-9. https://doi.org/10.1142/S0218348X09004284

[7]. Family F, Masters BR, Platt DE. Fractal pattern formation in human retinal vessels. North-Holland 1989 Sep;38(1): 98-103. https://doi.org/10.1016/0167-2789(89)90178-4

[8]. Landini G, Murray PI, Misson GP. Local connected fractal dimensions and lacunarity analyses of 60 degrees fluorescein angiograms. The Association for Research in Vision and Ophthalmology 1995 Dec;36(13): 2749-2755.

[9]. Caserta F, Eldred WD, Fernández E, Hausman RE, Stanford LR, Bulderev SV, Schwarzer S, Stanley HE. Determination of fractal dimension of physiologically characterized neurons in two and three dimensions. Elsevier 1995 Feb ;56(2): 133-144. https://doi.org/10.1016/0165-0270(94)00115-W PMid:7752679

[10]. Bordescu D, Paun MA, Paun VA, Paun VP. Fractal analysis of neuro imagistics. Lacunarity degree, a precious indicator in the detection of Alzheimer's disease 2018 May 3;80(4):309-320.

[11]. Khan MI, Wei J, Ronald M. Fractal analysis of tumor in brain MR images. Springer-Verlag New York, Inc. 2003 Mar;13(5): 352-362.
https://doi.org/10.1007/s00138-002-0087-9

[12]. De-Giorgio F, Ciasca G, Fecondo G, Mazzini A, Di Santo R, De Spirito M, Pascali VL. Post mortem computed tomography meets radiomics: a case series on fractal analysis of post mortem changes in the brain 2022 Mar;136(3):719-727.
https://doi.org/10.1007/s00414-022-02801-5
PMid:35239030 PMCid:PMC9005394

[13]. Kido S, Kuriyama K, Higashiyama M, Kasugai T, Kuroda C. Fractal analysis of small peripheral pulmonary nodules in thin-section CT: evaluation of the lung-nodule interfaces. J Comput Assist Tomogr. 2002 Jul ;26(4): 573-578.
https://doi.org/10.1097/00004728-200207000-00017
PMid:12218822

[14]. Paun VP, Agop M, Chen G, Focsa C. Fractal-Type Dynamical Behaviors of Complex Systems. Complexity 2018; 8029361 :1-3
https://doi.org/10.1155/2018/8029361

[15]. Nichita MV, Paun MA, Paun VA, Paun VP.Image Clustering Algorithms to Identify Complicated Cerebral Diseases. Description and Comparison. IEEE Access.2020;8:88434-88442.
https://doi.org/10.1109/ACCESS.2020.2992937

How to cite this article: Pooja I Shettannavar, Dishitha Kopoori, Vivek Chail, Vasudha Kulkarni. Fractal Analysis of Chest Radiographs Using Image-J-FIJI Software- A Pilot Study. Int J Anat Res 2024;12(4):9085-9092. **DOI:** 10.16965/ijar.2024.237